PHYSICAL REVIEW B VOLUME 29, NUMBER 4 15 FEBRUARY 1984

Elastic behavior under pressure of semiconducting SmS

Tu Hailing and G. A. Saunders
School of Physics, University of Bath, Claverton Down, Bath BA2 7AY, United Kingdom

H. Bach
Institut für Experimentalphysik IV, Ruhr Universität Bochum, D-4630 Bochum, West Germany
(Received 29 April 1983; revised manuscript received 15 August 1983)

From ultrasonic wave velocity measurements the hydrostatic pressure dependences of the second-order elastic constants of the semiconducting form of SmS have been obtained up to 6×10^8 Pa—just below the pressure (6.5×10^8 Pa) at which the isostructural first-order phase transition takes place. The major objectives have been to assess how the elastic behavior and the interatomic forces in SmS alter as the phase transition is approached. The results are compared and contrasted with those of $TmSe_{0.32}Te_{0.68}$, which also undergoes an isostructural transition but of closely second-order character. An isostructural volume collapse is associated with the identical irreducible representation η_0 $(=\eta_{11}+\eta_{22}+\eta_{33})$ and consequently bulk modulus instability. As SmS approaches the transition from the semiconducting side, its bulk modulus does decrease under pressure above about 3×10^8 Pa but not to a great extent. This behavior is in contrast with that of $TmSe_{0.32}Te_{0.68}$ whose bulk modulus decreases continuously under pressure to a small value at the transition. The elastic constant C_{12} reduces rapidly with pressure above about 3×10^8 Pa but, unlike that in $TmSe_{0.32}Te_{0.68}$, does not go through zero before the transition pressure is reached. C_{11} softens somewhat at high pressure, but C_{44} and $\frac{1}{2}(C_{11}-C_{12})$ show pressure dependences typical of rocksalt-structure crystals. The third-order elastic constants at atmospheric pressure have also been measured. Much of the largest third-order elastic constant is C_{111}, for which the nearest-neighbor repulsive forces are largely responsible. The anisotropy of the acoustic-mode Grüneisen γ parameters in the long-wavelength limit is explicable in terms of the strong influence of the nearest-neighbor repulsive forces on the third-order elastic constant C_{111}. At a pressure of 6×10^8 Pa (just below P_t), $\partial C_{11}/\partial P=-6.3$, $\partial C_{12}/\partial P=-22.8$, and $\partial B/\partial P=-17.3$—anomalous pressure dependences which arise (i) from enhanced interatomic binding due to an increase in the electron density in the delocalized d band as the gap between the highest f level and the bottom of the d band is reduced by application of pressure, and (ii) a reduction of the nearest-neighbor repulsive force at high pressure. This decrease in interatomic repulsive forces as P_t is neared is consistent with the breathing-mode model of the isostructural collapse. To provide an assessment of the elastic behavior under pressure in an alloy in the intermediate-valence state, the effects of the pressure on C_{11} and C_{44} for the metallic alloy $Sm_{0.576}Y_{0.424}S$ have also been measured; $\partial C_{11}/\partial P$ $(=+37.5)$ is large because the effect of pressure is to drive the crystal away from the transition, thereby stiffening the longitudinal mode.

I. INTRODUCTION

Samarium sulfide SmS undergoes a first-order isostructural phase transition at 6.5×10^8 Pa.[1] This transition has been associated with a bulk modulus instability;[2-4] to understand the nature of the transition it is necessary to ascertain the behavior of the interatomic forces as the transformation region is approached. To obtain information on this problem, the second-order elastic constants (SOEC) of SmS have been measured as a function of hydrostatic pressure into the vicinity of the phase transition. To enhance understanding of the interatomic forces, the third-order elastic constants (TOEC), which are usually dominated by the repulsive forces, have also been measured.

At atmospheric pressure SmS, which has the rocksalt structure, is an ionic semiconductor and is nominally $Sm^{2+}S^{2-}$. Samarium has an outer electronic configuration $4f^65s^25p^65d^06s^2$ and sulfur $3s^23p^4$. In rare-earth chalcogenides the d levels are broadened into a band, which is hybridized with the $6s$ band, while the localized $4f$ wave functions remain more or less the same as in the atom.[5-8] When hydrostatic pressure is applied to SmS, the lower of the crystal-field split d bands broadens and its energy gap relative to the highest f level decreases until the f level and the d-band edge cross.[9-11] A semiconductor-metal transition takes place near the pressure where the f-d gap tends to zero. This transition involves a delocalization of a $4f$ electron from the samarium ion ($4f^65d^0\rightarrow4f^55d^1$) as the valence state changes from 2+ towards 3+; the material changes dramatically in appearance from black to a golden metallic luster.[1,12,13] Owing to strong shielding by the $4f$ electrons of the outer $5s$ and $5p$ electrons from the nucleus, when a $4f$ electron is added to a rare-earth ion the ionic radius increases. Hence $Sm^{2+}(4f^6)$ has an almost 20% larger ionic radius than $Sm^{3+}(4f^5)$, and at the transition pressure P_t a large ($\sim10\%$) volume change occurs; this is accompanied by a sharp decrease in resistivity resulting from the delocalization of the f electron.[1] To account for the unusual magnetic properties of SmS above P_t, the metallic form has been considered to be in an intermediate-valence state.[14,15] This metallic state can also be induced by alloying with cations of a smaller size than Sm^{2+} (see Refs. 16—19) or with trivalent anions.[20]

The elastic behavior and the lattice dynamics of a compound in the intermediate-valence state can be most unusual. The second-order elastic constants (SOEC) of SmS itself[2–4] at atmospheric pressure are not atypical of a rocksalt-structure crystal, although, in common with the mixed ionic-covalent semiconductors PbTe and SnTe, C_{12} is smaller than C_{44}.[4] Alloys $Sm_{1-x}Y_xS$ with yttrium content x greater than approximately 0.15 ($=x_c$) are stabilized in the golden metallic form. The bulk modulus of these alloys is approximately linearly dependent upon the yttrium concentration x, and becomes very small as x approaches the critical concentration x_c which constitutes the stability limit of the metallic phase at atmospheric pressure and room temperature.[2,3] For a crystal to be stable its bulk modulus must be positive. The decrease in the bulk modulus as the yttrium concentration is taken towards x_c is consistent with the symmetry nonbreaking, volume collapse at P_t being a Cowley[21] type-O transition occurring through a bulk modulus instability.[20] Inspection of the elastic constant data[2,3] for the $Sm_{1-x}Y_xS$ alloys with x between approximately 0.25 and 0.4 shows that C_{12} is negative. This unusual characteristic has also been found for other intermediate-valence compounds $Tm_{0.99}Se$ (Ref. 22) and $TmSe_{0.32}Te_{0.68}$.[23] To follow the evolution of the intermediate valency, Boppart *et al.*[23] measured the ultrasonic wave velocities in $TmSe_{0.32}Te_{0.68}$ as a function of hydrostatic pressure through the pressure-induced continuous-phase transition to the metallic state at approximately 1.5 GPa. They observed that in the semiconducting state the bulk modulus goes to a small value and C_{12} becomes negative well below P_t. The elastic behavior under pressure of SmS has been examined previously,[4] but a complete set of elastic constants was not obtained throughout the existence region of the semiconducting phase. This has now been achieved. One objective has been to resolve the important question of whether there is any pretranslational softening of the acoustic modes in SmS. In contrast to the continuous nature of the phase transition in $TmSe_{0.32}Te_{0.68}$, that in SmS is strongly first order. Hence the SmS results enable an interesting comparison between the elastic behavior under pressure of a rocksalt crystal up to a discontinuous transition with that of $TmSe_{0.32}Te_{0.68}$ which undergoes a similar but almost continuous transformation.

The isentropic strain-energy density of a crystal is given by the power series expansion in Lagrangian strains $\underline{\eta}$ by

$$\rho_0 U(\underline{\eta}) = \tfrac{1}{2} C^S_{\alpha\beta\gamma\delta}\eta_{\alpha\beta}\eta_{\gamma\delta} + \tfrac{1}{6} C^S_{\alpha\beta\gamma\delta\epsilon\zeta}\eta_{\alpha\beta}\eta_{\gamma\delta}\eta_{\epsilon\zeta} + \cdots , \tag{1}$$

where $U(\underline{\eta})$ is the strain energy per unit mass, and ρ_0 is the density at atmospheric pressure. The coefficients

$$\rho_0[(\partial^3 U(S,\underline{\eta})/\partial\eta_{\alpha\beta}\partial\eta_{\gamma\delta}\partial\eta_{\epsilon\zeta})_S]_{\eta=0}$$

of the cubic term in strain are the adiabatic third-order elastic constants (TOEC) $C^S_{\alpha\beta\gamma\delta\epsilon\zeta}$ and quantify the vibrational anharmonicity to first order. Physical properties which depend upon thermal motion of the atoms are greatly influenced by anharmonicity, and knowledge of the TOEC provides quantitative understanding of thermal expansion, nonlinear acoustic behavior (phonon-phonon interactions), and particularly relevant in the present instance, crystal stability when a strain-tensor component is the order parameter corresponding to the phase change. An isostructural transition involving a bulk modulus instability is associated with a volume change η_0 $(=\eta_{11}+\eta_{22}+\eta_{33})$. The reduction of volume at P_t implies a collapse against the interionic repulsive forces: information about these forces should assist in developing a physical understanding of the influence of hydrostatic pressure on SmS. The pivotal importance of the TOEC in assessment of the interionic repulsive forces can be highlighted by consideration of a simplistic interatomic potential comprised of the sum of attractive and repulsive contributions, respectively,

$$\phi(R) = -A/R^n + B/R^m , \tag{2}$$

where R is the interatomic separation. As an elastic constant $C_{\alpha\beta\gamma\delta\epsilon\zeta,\ldots}$ of order a is the ath derivative $(\partial^a\phi(R)/\partial\eta_{\alpha\beta}\partial\eta_{\gamma\delta}\partial\eta_{\epsilon\zeta}\cdots)$ of the interatomic potential, successive differentiations of (2) show that the higher the order of the elastic constant, the greater is the influence on it of the repulsive term B/R^m, because (to ensure crystal stability) $m>n$. The shorter range and larger exponent of the repulsive potential usually require that those TOEC which dominate the third-order elasticity of a crystal are negative. It is to provide further information about the interionic repulsive forces in the semiconducting state that the TOEC of SmS have been measured.

The phonon dispersion curves of SmS have the form typical of those of an ionic semiconductor.[24] However, when they are compared with those of EuS, effects due to the smaller $4f$-$5d$ energy gap in SmS compared with that in EuS are observed: the LO branch is lowered, the bulk modulus is smaller. The lower energies at the Γ and L points have been ascribed, respectively, to an increased dipolar (Γ_{15}) and to an electronic deformability $(\Gamma_1)^+$, arising from virtual $4f$-$5d$ excitations, of the Sm ions. At the L point the "breathing" self-energy reduces the bulk modulus of SmS by about 15% as compared with that of EuS (Refs. 14, 25, and 26). The breathing deformability is linked closely with the isostructural transition.[26] The breathing mode involves simultaneous motion of the six sulfur ions surrounding a samarium ion along the lines joining these sulfur ions to the samarium: The relevant force constants are the nearest-neighbor ones corresponding to the attractive and repulsive forces between the unlike ions. Bulk modulus data have previously been used to assess the degree of ionicity involved in the attractive interatomic binding forces of the rocksalt structure rare-earth chalcogenides.[27] In a rocksalt-structure crystal the TOEC C_{111} is determined primarily by these forces and so can provide some information about them.

The ultrasonic signal is lost when SmS undergoes the transition. Hence to ascertain the effect of pressure on the elastic constants in the metallic phase, measurements have been made of the hydrostatic pressure dependences of C_{11} and C_{44} in a small (001) slice of $Sm_{0.576}Y_{0.424}S$. As the preliminary results obtained on this material add to the argument about the changing influence of repulsive forces on the elasticity of the rare-earth chalcogenides (by suggesting the resurgence of the nearest-neighbor repulsion on the other side of the transition) they are reported briefly here.

II. EXPERIMENTAL DETAILS

The single crystals of SmS and $Sm_{0.576}Y_{0.424}S$ were grown by a Bridgman technique. These materials cleave readily to expose $\{001\}$ faces so that [100] samples are easy to make, but specimens of a different orientation than this are singularly difficult to cut and polish. In fact the metallic alloy $Sm_{0.576}Y_{0.424}S$ crystal was in the form of a [001] plate which was too small to cut further into another specimen, so that the results on this material are restricted to those available from shear and longitudinal modes propagated down the [001] direction under the influence of hydrostatic pressure. In the earlier stages of the work on SmS the ultrasonic signals in the [110] direction were lost at quite low pressures;[4] however, this has been rectified with new samples: enough ultrasonic mode velocities could be measured to enable determination of all three SOEC as a function of hydrostatic pressure up to the near vicinity of the isostructural phase transition. Measurements of the ultrasonic velocity of the shear mode propagated in the [001] direction ($\rho v_s^2 = C_{44}$) were made[4] right up to the phase transition which occurred at 6.5×10^8 Pa, as reported by Jayaraman *et al.*[1] However, at that pressure the crystal disintegrated. As the rest of the crystals were needed for studies of the effects of uniaxial pressure, measurements have been restricted to an upper limit of 6×10^8 Pa. A pulse-echo overlap system was used to measure the changes induced by hydrostatic pressure on the ultrasonic wave velocity. Hydrostatic pressure was applied by a piston and cylinder equipment and uniaxial stresses using a screw press; the applied force was measured with a proving ring. To obtain the elastic stiffness constants of SmS under substantial hydrostatic pressure, an iterative correction procedure utilizing bulk modulus and compression $V(P)/V_0$ was used.

Determination of a complete set of TOEC requires accurate measurement of the initial slopes of the hydrostatic and uniaxial pressure dependences of ultrasonic wave velocities. To measure the small changes in ultrasonic wave velocity induced by uniaxial pressures of up to 2×10^6 Pa, an automatic frequency-controlled gated-carrier pulse superposition with a resolution of better than 1 part in 10^7 (Ref. 28) was employed. To take into account the changes in crystal dimensions and density with pressure, the "natural velocity" W method[29] was used, the experimental data for the pressure-induced change in the ultrasonic wave transit time being converted to change of natural velocity (W/W_0-1).

III. EXPERIMENTAL RESULTS AND THEIR PHYSICAL SIGNIFICANCE

The SOEC of SmS measured at 293 K are compared with those[23] of $TmSe_{0.32}Te_{0.68}$, which also undergoes a semiconductor-to-metallic transition, in Table I. The SOEC at atmospheric pressure, which have been given before,[4] are in reasonable agreement with those obtained by other workers.[2,3] Similarities in interatomic binding usually lead to a general pattern of SOEC for isostructural crystals. For rocksalt-structure crystals, it is usual for C_{11} to be several times as large as C_{44}; this is so for SmS. The elastic constants resemble those of the IV-VI compound semiconductors PbTe [$C_{11}=1.053$, $C_{12}=0.070$, and $C_{44}=0.132$, in units of 10^{11} N m^{-2} (Ref. 30)], and SnTe ($C_{11}=1.043$, $C_{12}=0.0178$, and $C_{44}=0.113$ (Ref. 30). This is consistent with mixed ionic-covalent binding forces in the semiconducting form of SmS.[31] For a more nearly ideal ionic crystal such as NaCl the forces are central so that the Cauchy relation ($C_{12}=C_{44}$) holds. However, for SmS, like PbTe and SnTe, there is a considerable

TABLE I. The elastic properties of SmS at room temperature. Units of the stiffnesses are 10^{11} N m^{-2} and those of compressibility are 10^{-11} m^{2}N^{-1}. The parameters for $TmSe_{0.32}Te_{0.68}$ have been extracted from the data given in Ref. 23. The elastic constants at atmospheric pressure have been given previously in Ref. 4.

		SmS			$TmSe_{0.32}Te_{0.68}$
		Hydrostatic pressure P			
			3×10^8 Pa	6×10^8 Pa	
		1 Pa	(3 kbar)	(6 kbar)	1 Pa
Elastic stiffness	C_{11}	1.270	1.301	1.282	0.974
	C_{12}	0.12	0.115	0.047	0.0367
	C_{44}	0.2690	0.2688	0.2685	0.218
	$C'=\frac{1}{2}(C_{11}-C_{12})$	0.575	0.593	0.618	0.469
Bulk modulus	B	0.503	0.510	0.458	0.37
Anisotropy ratio	C_{44}/C'	0.47	0.45	0.43	0.43
Volume compressibility	K_v	1.988	1.96	2.183	2.7
Linear compressibility	K_a	0.66	0.67	0.75	0.9
Lattice parameter	a (10^{-10} m)	5.970	5.958	5.945	
Compression	$V(P)/V_0$	0.994		0.987	

deviation with $C_{12} < C_{44}$, such a deviation being traditionally associated with covalency. The elastic constants obtained at 3×10^8 and 6×10^8 Pa are also given in Table I. At 6×10^8 Pa, which is close to the phase transition at 6.5×10^8 Pa, the deviation from the Cauchy relation is substantially greater than at atmospheric pressure suggesting that the interatomic forces become more decentralized as the transition is approached. These findings conform with the breathing-shell model which suggests that the breathing force deformability should result in $\Delta(C_{12}-C_{44})<0$,[24] an effect that should be enhanced near P_t.

The hydrostatic pressure dependences of the elastic stiffness constants C_{11}, C_{44}, and $C'=[\frac{1}{2}(C_{11}-C_{12})]$ measured up to 6×10^8 Pa are shown in Fig. 1. There is no significant acoustic shear mode softening in SmS as it approaches P_t. The modulus $\frac{1}{2}(C_{11}-C_{12})$, associated with shear in a $\langle 1\bar{1}0\rangle$ direction in a $\{110\}$ plane, increases almost linearly with pressure in the normal way. Although C_{44} does decrease slightly right up to P_t,[4] this is not behavior peculiar to SmS. Small values of $\partial C_{44}/\partial P$ are the norm for rocksalt-structure crystals. As the pressure derivatives $\partial C_{IJ}/\partial P$ collected in Table II indicate, it is not uncommon for $\partial C_{44}/\partial P$ to be negative. The influence of volume conserving shears is not of central importance for the isostructural volume collapse.[32] The modulus C_{11}, obtained from velocity measurements of the longitudinal ultrasonic mode propagated down the [100] direction, is unusual in that it decreases with pressure above approximately 3×10^8 Pa: there is some softening of the longitudinal-acoustic mode.

Knowledge of the bulk modulus is central to an understanding of the interatomic binding forces of SmS. The bulk modulus measured at atmospheric pressure (Table I) is in reasonable agreement with values obtained previously for single crystalline material: $0.48\pm0.05\times10^{11}$ N m^{-2} from bulk compressibility measurements under hydrostatic pressure,[10] 0.475×10^{11} N m^{-2} from elastic constant data.[3] The bulk modulus of both phases has been estimated from lattice-parameter determinations made under hydrostatic pressure up to 70×10^8 Pa;[33] a linear fit to the data points for the semiconducting phase up to the phase-transition pressure 6.5×10^8 Pa gave a bulk modulus of $(0.42\pm0.03)\times10^{11}$ N m^{-2}. The consensus is that the bulk modulus of SmS is significantly less than that of EuS (Ref. 27) as a result of the "breathing self-energy."[14,25,26] Since it has not proved possible to make ultrasonic measurements at pressures beyond the transition point, the bulk modulus (0.52×10^{11} N m^{-2} at the transition pressure) and its large pressure derivative B_f' ($+11\pm2$) measured by Keller and his co-workers[33] for the high-pressure form are particularly interesting. Alloying SmS with sufficient smaller size cations such as Y^{3+} to produce a material in the intermediate-valence state does not actually simulate the high-pressure form of SmS as their bulk modulus measurement demonstrates: that of $Sm_{1-x}Y_xS$ with x close to x_c (~0.15) being more than an order of magnitude smaller.[2,3] The large value of $+37.5$ found here (Table III) for $\partial C_{11}/\partial P$ for the $Sm_{0.576}Y_{0.424}S$ crystal suggests that $\partial B/\partial P$ is even larger in the "chemically stabilized" $Sm_{1-x}Y_xS$ alloys than in the metallic phase of SmS itself.

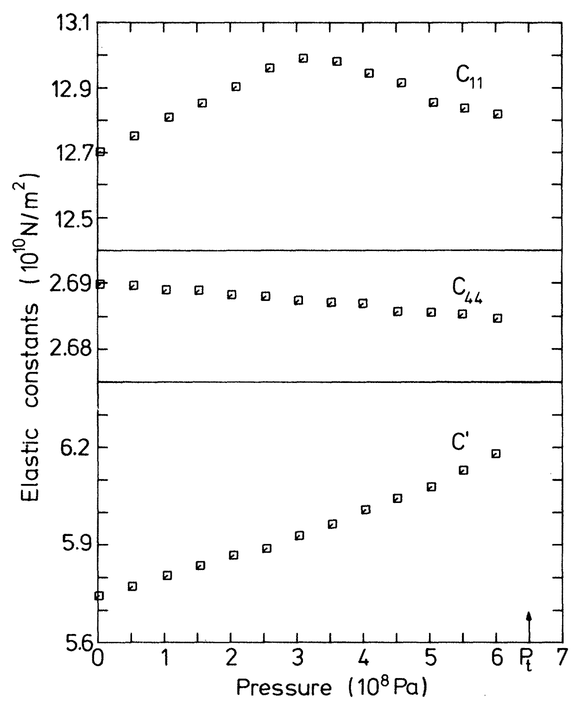

FIG. 1. Hydrostatic pressure dependences of the elastic stiffness moduli C_{11}, C_{44}, and C' $[=\frac{1}{2}(C_{11}-C_{12})]$ of SmS.

It is useful to compare the SOEC of SmS with those made under pressure of $TmSe_{0.32}Te_{0.68}$ (Ref. 23) in which the pressure-induced transition to an intermediate valence, metallic state takes place at 1.5 GPa. As the pressure is

TABLE II. Hydrostatic pressure derivatives of SOEC for SmS at atmospheric pressure and 6×10^8 Pa in comparison with those of other crystals with the rock-salt structure.

	$\partial C_{11}/\partial P$	$\partial C_{12}/\partial P$	$\partial C_{44}/\partial P$	$\partial C'/\partial P$	$\partial B/\partial P$
SmS $P=1$ Pa	$+10.4$	-1.6	-0.08	$+6.0$	$+2.4$
$P=6\times10^8$ Pa	-6.3	-22.8	-0.08	$+8.2$	-17.3
$TmSe_{0.32}Te_{0.68}$	$+7$	-4	$+0.4$	$+5.5$	-0.3
PbTe (30)	$+13.4$	$+1.0$	$+0.19$	$+5.9$	$+5.1$
SnTe (30)	$+14.0$	$+1.5$	$+0.14$	$+6.2$	$+5.7$
NaCl (32)	$+11.7$	$+2.1$	$+0.37$	$+4.8$	$+5.3$
KCl (32)	$+12.8$	$+1.6$	-0.39	$+5.6$	$+5.3$
KBr (32)	$+13.5$	$+1.6$	-0.30	$+6.0$	$+5.6$

TABLE III. The elastic properties of a single crystal of $Sm_{0.576}Y_{0.424}S$ at 293 K are given in (a). In (b), the parameters have been estimated by including data obtained from Refs. 2 and 3. Errors in C_{11} and C_{44} are $\pm 2\%$ and in $\partial C_{11}/\partial P$, $\partial C_{44}/\partial P$, $(C_{111}+2C_{112})$, and $(C_{144}+2C_{166})$ they are $\pm 6\%$.

(a)	
$C_{11}=1.52\times 10^{11}$ Nm^{-2}	$\partial C_{11}/\partial P=37.5$
$C_{44}=0.31\times 10^{11}$ Nm^{-2}	$\partial C_{44}/\partial P=-0.83$
$C_{111}+2C_{112}=-35.0\times 10^{11}$ Nm^{-2}	
$C_{144}+2C_{166}=-0.46\times 10^{11}$ Nm^{-2}	
Lattice parameter $a_0=5.62$ Å	
(b)	
$C_{12}\simeq -0.32\times 10^{11}$ Nm^{-2}	
$C'\simeq +0.92\times 10^{11}$ Nm^{-2}	
Anisotropy ratio $\simeq C_{44}/C'\simeq 0.34$	
Bulk modulus $B\simeq 0.29\times 10^{11}$ Nm^{-2}	
Compressibility $\chi \simeq 3.45\times 10^{-11}$ m^{2}N^{-1}	

increased on $TmSe_{0.32}Te_{0.68}$, C_{44} increases slightly, $\frac{1}{2}(C_{11}-C_{12})$ rather more so and with a continuously steepening gradient (because C_{12} becomes more negative). The longitudinal-mode softening at high pressures is also evident for this material, the pressure dependence of C_{11} changes slope above approximately 0.5 GPa. The pressure-induced changes in the elastic constants of $TmSe_{0.32}Te_{0.68}$ are larger than those in SmS especially as the transition is neared, when the continuous nature of the transition in $TmSe_{0.32}Te_{0.68}$ becomes apparent. The behaviors of C_{12} and the bulk modulus B, which have been followed through the continuous transition in $TmSe_{0.32}Te_{0.68}$, are most unusual. C_{12}, which is small and positive at atmospheric pressure (Table I), goes negative above approximately 0.6 GPa—Poisson's ratio then becomes anomalously negative. The bulk modulus softens under pressure, reducing to a small value at P_t. There are two ways by which the bulk modulus could go towards zero: either (i) both C_{11} and C_{12} vanish or (ii) if C_{12} is negative and the magnitude of $2C_{12}$ becomes equal to C_{11}.[22] The latter case is responsible for the small bulk modulus near P_t in $TmSe_{0.32}Te_{0.68}$, this decrease of the bulk modulus being consistent with enhancement of the breathing deformability as the valence transition is approached.[23]

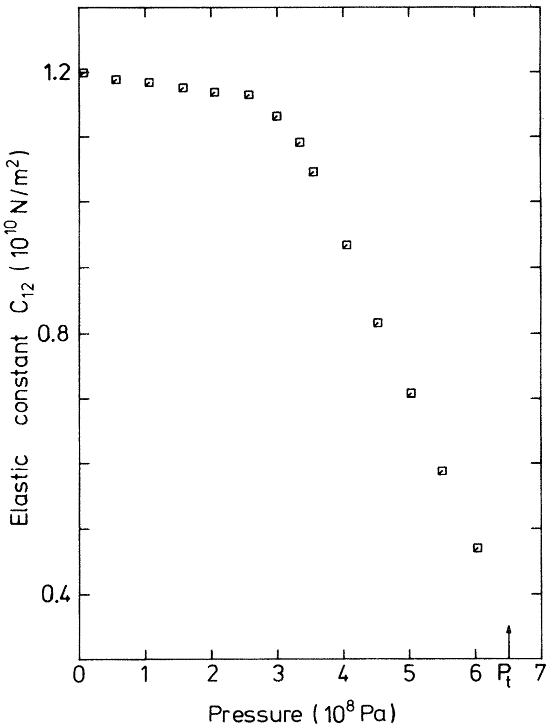

FIG. 2. Hydrostatic pressure dependence of C_{12} for SmS.

The strongly first-order character of the phase transition in SmS, as distinct from the continuous nature of that in $TmSe_{0.32}Te_{0.68}$, results in different behavior of C_{12} and B for the two materials. Thus although C_{12} decreases approximately linearly with pressure above about 3×10^8 Pa for SmS, it remains positive up to 6×10^8 Pa (Fig. 2); a linear extrapolation gives C_{12} equal to $+0.35\times 10^{10}$ N m^{-2} at P_t. The bulk modulus behaves similarly (being dependent upon the change in C_{12}) and extrapolates to 4.5×10^{10} N m^{-2} at P_t: still, however, a large value compared with that (6×10^9 N m^{-2}) of $TmSe_{0.32}Te_{0.68}$ near P_t.[23]

For a cubic crystal the elastic strain energy (which must be a positive definite for stability) is given by[34,35]

$$\begin{aligned}\phi=&\tfrac{1}{6}(C_{11}+2C_{12})(\eta_0^0)^2+\tfrac{1}{4}(C_{11}-C_{12})(\eta_1^2+\eta_2^2)+\tfrac{1}{2}C_{44}(\eta_3^2+\eta_4^2+\eta_5^2)\\&+\tfrac{1}{54}(C_{111}+6C_{112}+2C_{123})(\eta_0^0)^3+\tfrac{1}{12}(C_{111}-C_{123})\eta_0^0(\eta_1^2+\eta_2^2)\\&+\frac{1}{24\sqrt{3}}(C_{111}-3C_{112}+2C_{123})\eta_1(\eta_1^2-3\eta_2^2)+\tfrac{1}{6}(C_{144}+2C_{155})\eta_0^0(\eta_3^2+\eta_4^2+\eta_5^2)\\&+\frac{1}{4\sqrt{3}}(C_{144}-C_{155})\eta_1(2\eta_5^2-\eta_4^2-\eta_3^2)+\tfrac{1}{4}(C_{144}-C_{155})\eta_2(\eta_3^2-\eta_4^2)+C_{456}\eta_3\eta_4\eta_5\ ,\end{aligned}\quad (3)$$

where the eigenvectors, in terms of Lagrangian strain-tensor components η_{ij}, are $\eta_0=\eta_{11}+\eta_{22}+\eta_{33}$, $\eta_1=3^{-1/2}(2\eta_{33}-\eta_{22}-\eta_{11})$, $\eta_2=\eta_{33}-\eta_{11}$, $\eta_3=\eta_{23}$, $\eta_4=\eta_{13}$, and $\eta_5=\eta_{12}$. An isostructural transition is associated with the identical irreducible representation η_0 which relates to a volume change only—there is no symmetry breaking and the distortion is not carried by an acoustic wave. The change in volume at the transition ensues through a bulk modulus instability (Fig. 3), which develops continuously in $TmSe_{0.32}Te_{0.68}$, but occurs

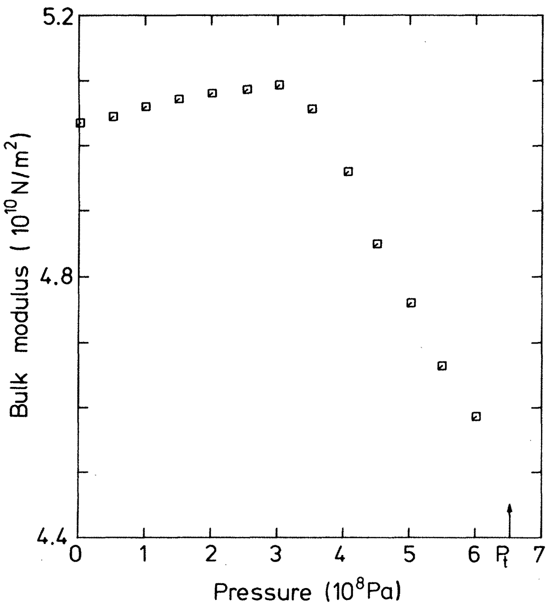

FIG. 3. Hydrostatic pressure dependence of the bulk modulus.

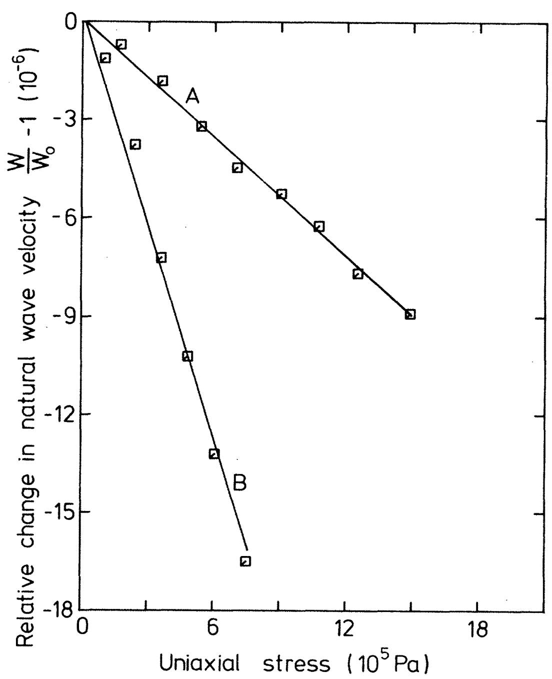

FIG. 4. Relative change, induced by application of a uniaxial pressure on the [010] direction, the natural velocity of *A*, a longitudinal ultrasonic wave, and *B*, a shear ultrasonic wave propagated in the [100] direction of SmS.

discontinuously in SmS. The pressure measurements of the elastic constants enable a quantitative determination of the coefficients of η_0 in the strain-free-energy expansion. Since

$$\frac{\partial B}{\partial P}=-\frac{C_{111}+6C_{112}+2C_{123}}{9B}\ , \tag{4}$$

the terms out to third order in η_0 can be shown, using Eq. (3), to be

$$\begin{aligned}\phi(\eta_0)&=\frac{1}{2}B\eta_0^2-\frac{1}{6}B\left[\frac{\partial B}{\partial P}\right]\eta_0^3\\ &=2.29\times10^{10}\eta_0^2+1.3\times10^{11}\eta_0^3 \text{ for SmS at } P_t\ .\end{aligned} \tag{5}$$

Hence, the strain-free energy in the identical irreducible representation η_0 is dominated by the quadratic term when η_0 is a small quantity. This is quite different behavior from that found at a soft acoustic-phonon mode transition of nearly second-order character where the higher-order terms in the symmetry-breaking eigenvector become increasingly important as the phase transition is approached and the anharmonicity of the soft mode drives the structural transformation.[34,35]

The changes induced by uniaxial pressure applied in the [010] direction on the velocity of shear and longitudinal ultrasonic wave propagated down the [001] direction are shown in Fig. 4. The measured TOEC calculated from the hydrostatic and uniaxial pressure dependences of the ultrasonic wave velocities are compared, as there are no other sets of TOEC for an R^{2+} monochalcogenide, with those of some rocksalt-structure crystals in Table IV. For all these crystals C_{111} has a large negative value while the other TOEC are about an order of magnitude smaller.

The hydrostatic pressure dependences of the velocities of ultrasonic waves propagated down the [001] direction of a single crystal of the gold-colored metallic $Sm_{0.576}Y_{0.424}S$ were also measured. The values for C_{11} and C_{44} (Table III) are in reasonable agreement with those of other alloys in the series $Sm_{1-x}Y_xS$.[18,19] C_{12} is negative for these metallic alloys[18,19] (so that Poisson's ratio

TABLE IV. The experimental values of the TOEC of SmS at room temperature in comparison with those of other rocksalt-structure crystals. Units are 10^{11} Nm^{-2}. The sources of the TOEC data of crystals other than SmS can be found in Ref. 30.

	C_{111}	C_{112}	C_{123}	C_{144}	C_{166}	C_{456}
SmS	−28.2	+4.9	−2.85	+0.25	−0.95	0
PbTe	−18.5	+0.35	−0.97	+0.44	−0.98	+0.12
NaCl	−8.4	−0.50	+0.46	+0.29	−0.60	+0.26
NaF	−14.8	−2.70	+2.80	+0.46	−1.14	0
KCl	−7.26	−0.24	+0.11	+0.23	−0.26	+0.16

should be negative) like those of $Tm_{0.99}Se$ (Ref. 22) and $TmSe_{0.32}Te_{0.68}$.[23] The effect of hydrostatic pressure on these [001] modes in the metallic $Sm_{0.576}Y_{0.424}S$ alloy is to decrease the shear-wave velocity slightly and to increase considerably that of the longitudinal wave (Fig. 5). As a result, $\partial C_{44}/\partial P$ has a fairly small negative value (Table III) like that of semiconducting SmS (Table II). The corresponding volume conserving shear has no more unusual effects in the intermediate valent state of the alloy than it has in the semiconducting state of SmS. However, $\partial C_{11}/\partial P$ has a very large positive value (Table III) [about three times that which is normal in a rocksalt-structure crystal (Table II)]. A large value of $\partial C_{11}/\partial P$ represents a pronounced pressure-induced stiffening against compression and thus corresponds to an enhanced magnitude of $\partial B/\partial P$, which should also be large in the alloys. Application of pressure in the metallic state takes a crystal away from the phase transition.

IV. RELATIVE CONTRIBUTIONS FROM ATTRACTIVE AND REPULSIVE FORCES TO THE ELASTIC CONSTANTS OF SmS

At atmospheric pressure the SOEC, their hydrostatic pressure derivatives, and the TOEC of SmS follow a similar pattern to those of the rocksalt-structure alkali halides.

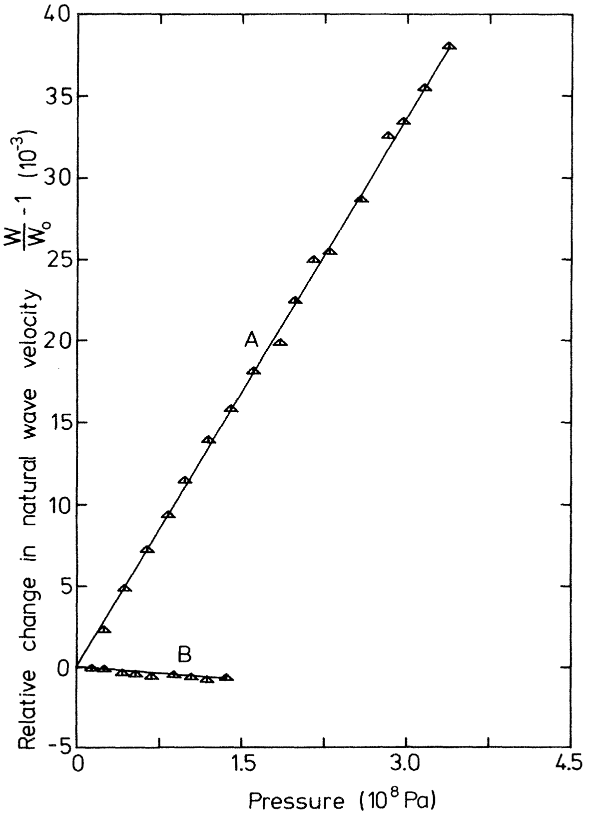

FIG. 5. Relative change induced by hydrostatic pressure on the natural wave velocity of ultrasonic modes propagated down the [001] direction in a $Sm_{0.576}Y_{0.424}S$ crystal. Line A corresponds to the longitudinal mode $[V_L=(C_{11}/\rho)^{1/2}]$ and line B to the shear mode $[V_S=(C_{44}/\rho)^{1/2}]$.

Anderson and Nafe[36] found that there is an empirical scaling law between the bulk modulus B in terms of the equilibrium interionic distance for a given class of related compounds. The data for B_0 and r_0 for the $R^{2+}X$ and R^{3+} compounds fall on two separate straight lines, which are parallel to that of the alkali halides, demonstrating the important role played by ionic binding in these compounds. By comparing the bulk modulus ratio for a rare-earth chalcogenide to the alkali halide with the same unit-cell volume, the effective ionic charges $Z_{\mathrm{eff}}=(Z_1^*Z_2^*)^{1/2}$ of the constituent ionic species have been estimated as 1.70 ± 0.03 and 1.85 ± 0.05 for R^{2+} and R^{3+} compounds, respectively.[27] These effective ionic charges are somewhat smaller than the values of 2 and 2.45, respectively, which would be expected from the valence products. SmS was not included in this study; however, with the bulk modulus of 0.503×10^{11} $\mathrm{N\,m^{-2}}$ (Table I) and the unit-cell volume a_0^3 equal to 266 $\mathrm{\AA}^3$, SmS comes just below the straight line for the semiconducting R^{2+} chalcogenides. Since this behavior is roughly consistent with the Born-Mayer central-force model, it is of interest to see how closely such a model describes the second- and third-order elastic constants of SmS. A detailed study of this question clearly shows that an ionic model cannot be used in this way. This is not unexpected since central forces require the Cauchy conditions: (i) on SOEC $C_{12}=C_{44}$; (ii) on TOEC $C_{123}=C_{456}=C_{144}$; $C_{112}=C_{116}$; and for SmS $C_{44}\sim2C_{12}$ at atmospheric pressure and $C_{44}\sim5C_{12}$ at 6 kbar. While all five TOEC involved are small, the Cauchy requirements on third-order elasticity are not obeyed.

The lattice energy of a rigid-ion crystal with Coulombic binding and a Born-Mayer—type central-force repulsive interaction between neighbors is

$$\phi_{\mu\nu}(r)=-N[(\alpha Z_1Z_2w/r)-b\exp(-r/\rho)]\ . \qquad (6)$$

Here α is the Madelung constant, which equals 1.747 56 for the rocksalt structure. For a mixed ionic-covalent compound the model suffers from its failure to take account of noncentral, nonionic forces, and so its predictions can only be qualitative. The attractive forces are balanced by the repulsive forces, which oppose interpenetration of the ions so that the crystal does not collapse but exists with an equilibrium separation r_0 between the neighboring cations and anions. Typically these repulsive forces reduce the binding energy by about 10%. The repulsive parameter ρ can be determined from the volume derivative of the equation of state, which gives the condition for crystal equilibrium and compressibility as

$$\delta=\frac{r_0}{\rho}=\frac{9cr_0^4}{K_v\alpha Z_{\mathrm{eff}}^2e^2}+2\ , \qquad (7)$$

where c is 2 for the rocksalt structure. Hence ρ is obtained from the experimental values of the nearest-neighbor distance r_0 and the compressibility K_v. Using an effective charge Z_{eff} $[(=Z_1^*Z_2^*)^{1/2}]$ of 1.7 determined[27] for the R^{2+} monochalcogenides gives a value of 0.365 for ρ for SmS.

On the basis of the Born model formulated by Krishnan and Roy[31] these values of Z_{eff} and ρ lead to 0.93×10^{11}

$\mathrm{N\,m^{-2}}$ and 0.29×10^{11} $\mathrm{N\,m^{-2}}$ for C_{11} and C_{44}, respectively. The assumption that an effective net charge, determined by Z_{eff}, can be ascribed to each atom can be viewed as an attempt to resolve the difficulty that the ionic and overlap contributions cannot be isolated and defined. In spite of the inadequacy of the model some useful conclusions can be drawn about the elastic behavior and interatomic binding in SmS. For C_{11} the repulsive contribution W_R from nearest neighbors is about twice the long-range Madelung term. TOEC are even more dependent upon repulsive forces. Expressions for the TOEC (at 0 K) of rocksalt-structure crystals have been obtained by Ghate[38] in the Born-Mayer model, including the short-range repulsive interactions up to next-nearest neighbors. For ions with an effective valence Z_{eff} his expression for the largest TOEC C_{111} can be reformulated as

$$C_{111}=+9.2375\times10^{10}\frac{Z_{\mathrm{eff}}^2e^2}{r_0^4}-\frac{\phi(r_0)}{\rho}\left[\frac{3}{r_0^2}+\frac{3}{\rho r_0}+\frac{3}{\rho^2}\right]-\frac{\phi(\sqrt{2}r_0)}{2\rho}\left[\frac{3\sqrt{2}}{r_0^2}+\frac{6}{\rho r_0}+\frac{2\sqrt{2}}{\rho^2}\right]. \qquad (8)$$

Here the second and third terms arise from repulsive interactions between nearest and next-nearest neighbors, respectively. For SmS taking Z_{eff} as 1.7 and the repulsive parameter ρ as 0.365, we find that the Madelung contribution to C_{111} is $+8.6\times10^{11}$ $\mathrm{N\,m^{-2}}$, the nearest-neighbor repulsive term gives -21.0×10^{11} $\mathrm{N\,m^{-2}}$ while the next nearest-neighbor repulsion provides only -0.9×10^{11} $\mathrm{N\,m^{-2}}$. C_{111} has a large negative value because it is dominated by the repulsive forces between nearest-neighbor (samarium and sulfur) atoms which give a contribution several times larger than that of the attractive forces. Owing to the short range of the repulsive forces, the contribution to C_{111} from repulsion between next-nearest neighbor (like atoms) is about 2 orders of magnitude smaller than that from the nearest neighbors. The ionic model breaks down for C_{112} and C_{123} for which it even predicts the wrong sign; C_{112} is dominated by forces between next-neighbor ions.

In the rocksalt structure a shear distortion ϵ_{yz} $(=\partial v/\partial z+\partial w/\partial y)$, where v is a displacement in the y direction and w is one in the z direction, is associated with C_{44} and C_{456}. This shear corresponds to sliding of planes of constant z over each other in the y direction so that there is no change in nearest-neighbor distance to first order in strain and no nearest-neighbor repulsive contribution to these elastic constants. Hence C_{456} is very small (and difficult to measure).

It is customary to discuss the anharmonic behavior of crystals in terms of generalized Grüneisen parameters which measure the strain dependence of the lattice vibrational frequencies $\omega_p(\underline{q})$ resulting from hydrostatic pressure-induced changes in the lattice potential. In the elastic continuum model at the long-wavelength limit the acoustic-mode Grüneisen parameters $\gamma(p,\underline{N})$, where p denotes the branch and $\underline{N}$ is a unit vector in the propagation direction, are given by[39]

$$\gamma(p,\underline{N})=-(1/6w)(3B+2w+k) \qquad (9)$$

where

$$w(p,\underline{N})=C_{11}K_1+C_{44}K_2+C_{12}K_3\ ,$$
$$k(p,\underline{N})=C_1K_1+C_2K_2+C_3K_3\ ,$$

with

$$K_1(p,\underline{N})=N_1^2U_1^2+N_2^2U_2^2+N_3^2U_3^2\ ,$$
$$K_2(p,\underline{N})=(N_2U_3+N_3U_2)^2+(N_3U_1+N_1U_3)^2+(N_1U_2+N_2U_1)^2\ ,$$
$$K_3(p,\underline{N})=2(N_2N_3U_2U_3+N_3N_1U_3U_1+N_1N_2U_1U_2),$$
$$C_1=C_{111}+2C_{112}\ ,$$
$$C_2=C_{144}+2C_{166}\ ,$$
$$C_3=C_{123}+2C_{112}\ .$$

N_i and U_i are the direction cosines for the propagation and polarization directions. Since these mode Grüneisen γ parameters relate only to hydrostatic pressure, they can be determined from the elastic constants and their hydrostatic pressure derivatives alone. The three required TOEC combinations C_1, C_2, and C_3, evaluated from the measured hydrostatic pressure derivatives of the SOEC are given at atmospheric pressure and 6×10^8 Pa (just below P_t) in Table V. The orientation dependences of the acoustic-mode Grüneisen γ parameters, $\gamma(p,\underline{N})$, for each of the acoustic branches of the phonon dispersion curves at the Brillouin-zone center [Fig. 6(a)] have been obtained at these two pressures by substituting the values of C_1, C_2, and C_3 into Eq. (9); the mode velocities for a given propagation direction $\underline{N}$ have been computed by solving the Christoffel equations. At atmospheric pressure the orientation dependence of $\gamma(p,\underline{N})$ resembles that of the rocksalt-structured alkali halides and of PbTe and SnTe.[30] Consider the $\gamma(p,\underline{N})$ for acoustic modes propagating along a fourfold $\langle001\rangle$ direction. For the longitudinal mode $\gamma(p,\underline{N})$ is large ($+1.83$) but that for the degenerate shear [polarization vector in the (001) plane] is small and negative (-0.28). The physical reasons for this are as follows. The mode equation for $\gamma_L[001]$ involves C_1 $(=C_{111}+2C_{112})$ which is large and negative. Therefore, $\gamma_L[001]$ is dominated by C_{111}. Now C_{111} is the largest

TABLE V. Experimental values of the TOEC combinations available from the hydrostatic pressure dependences of the elastic stiffness constants. Units are 10^{11} $\mathrm{Nm^{-2}}$. Data at atmospheric pressure have been given previously in Ref. 4; data for $\mathrm{TmSe_{0.32}Te_{0.68}}$ have been calculated from results in Ref. 23.

	SmS Atmospheric pressure	6×10^8 Pa	$\mathrm{TmSe_{0.32}Te_{0.68}}$ Atmospheric pressure
$C_{111}+2C_{112}$	-18	$+6.8$	-7.9
$C_{123}+2C_{112}$	-3.8	$+36.2$	-5.1
$C_{144}+2C_{166}$	-1.6	-1.7	-1.2
$\bar{\gamma}_H$	$+1.10$	-0.34	$+0.75$

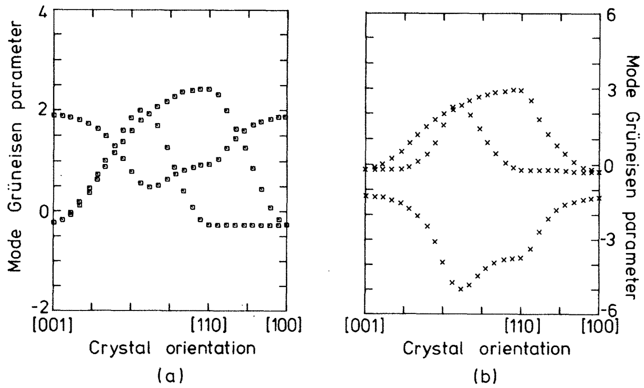

FIG. 6. Long-wavelength acoustic-mode Grüneisen parameters of SmS as a function of mode propagation direction (a) at atmospheric pressure and (b) at 6×10^8 Pa.

TOEC because of the predominance of the nearest-neighbor repulsive force: these also dominate $\gamma_L[001]$. The resistance of the nearest-neighbor ions to being pushed together causes the frequency and energy of the [001] longitudinal mode to be quite strongly volume dependent. In contrast, for the shear wave propagating in the [001] direction $K_1=0$, so that C_{111} is not involved in the expression (9) for $\gamma_T[001]$ while C_2 $(=C_{144}+2C_{166})$, which is much smaller than C_1 $(=C_{111}+2C_{112})$, is. Hence $\gamma_T[001]$ is much smaller than $\gamma_L[001]$ because the nearest-neighbor repulsive force does not influence it. The transverse mode propagating along the [001] direction in the rocksalt structure is one in which the z planes of atoms vibrate, as a unit, perpendicular to direction of nearest-neighbor bonds not in the plane. All the changing bond lengths would increase, if the atom planes were to move rigidly, so that the Grüneisen parameter $\gamma_T[001]$ can be slightly negative, as indeed it is for SmS. Nearly zero, often negative, $\gamma_T[001]$ values are the norm for rocksalt structure IV-VI and alkali halides.[30] In general, the magnitudes of $\gamma(p,\underline{N})$ for SmS at atmospheric pressure can be accounted for by considering whether a component of C_{111}, and thus of the nearest-neighbor repulsive force, is included in them.

As the hydrostatic pressure is increased towards that at which the phase transition takes place, SmS and $\mathrm{TmSe_{0.32}Te_{0.68}}$ have similar pressure derivatives of the SOEC (Table II). For both materials $\partial B/\partial P$, $\partial C_{11}/\partial P$, and $\partial C_{12}/\partial P$ become large and negative, while the shear mode derivatives remain similar to their values at atmospheric pressure. These hydrostatic pressure dependences give the three TOEC combinations in Table V. The change in sign from negative to positive for the third-order combinations $C_{111}+2C_{112}$ and $C_{123}+2C_{112}$ as both materials are squeezed from atmospheric pressure to just below their transitions shows that the balance between the attractive and repulsive contributions to the interatomic binding has altered completely near P_t. The positive values of both $C_{111}+2C_{112}$ and $C_{123}+2C_{112}$ near P_t indicate that attractive interatomic forces now dominate the third-order elasticity. This can be brought about by two effects, both of which may be operating. In the semiconducting form of SmS the energy separation ΔE_g ($\sim$0.2 eV) between the highest occupied f levels and the bottom of the $5d$ band is reduced considerably $[d(\Delta E_g)/dP=10$ meV/10^8 Pa (Ref. 40)] when pressure is applied. While the f levels are more or less atomic in character, the d levels are broadened into a band, hybridized with the $6s$ band. Hence with increasing pressure the probability of promotion into the d band becomes greater and the consequent delocalization of the electrons increases the shared electron contribution to the interatomic binding. An increase in electron sharing will cause C_{112} to become even more positive, as the large positive value found for $C_{123}+2C_{112}$ (Table V) near P_t suggests. The enhancement of d-band electron density as P_t is approached should have a smaller effect on the attractive interatomic contributions to C_{111} than on C_{112} because the ionic binding contribution to C_{111} will become smaller as its electron sharing contribution gets larger: These two influences act in the opposite sense. The second effect which could make $C_{111}+2C_{112}$ become more positive under high pressure is a decrease in the repulsive force between nearest neighbors as the transition is approached. This would drive C_{111} in the positive direction. It would also be just the effect to enable the transition to take place. As the nearest-neighbor repulsive force decreases, the breathing mode, in which the six sulfur ions move simultaneously towards (and then away from) the samarium ion which they surround, would become much easier. The transition occurs when the enhancement of the attractive forces combined with the reduction of the nearest-neighbor repulsive forces becomes sufficient to allow the crystal to collapse.

Thus the positive values of the TOEC combinations $C_{111}+2C_{112}$ and $C_{123}+2C_{112}$ near P_t provide evidence for the enhancement of the crystal instability against the breathing mode which drives the isostructural transition in SmS. The influence of the lattice instability near P_t on the mode Grüneisen parameters also attests to this: The $\gamma(p,\underline{N})$ for all the longitudinal and quasilongitudinal modes are anomalously negative, as these modes soften under pressure [Fig. 6(b)]. The shear-mode γ parameters essentially retain their atmospheric pressure characteristics.

The hydrostatic pressure derivatives of the SOEC and the TOEC have provided detailed information of the elastic behavior of the semiconducting form of SmS and have led to knowledge of the way in which the interatomic forces change as the densification phase transition is approached. The large volume decreases which onsets at the transition and the consequent degradation of the crystal have precluded study of the elastic properties of the low-volume SmS itself. However, the preliminary results obtained for the $\mathrm{Sm_{0.576}Y_{0.424}S}$ alloy crystal (Table III, Fig. 5) provide an indication of the elastic behavior under pressure in the metallic modification. The large positive $\partial C_{11}/\partial P(+37.5)$ and resultant large negative value $(-35.0\times10^{11}\ \mathrm{N\,m^{-2}})$ (Table III) found for $C_{111}+2C_{112}$ for this metallic alloy indicate that C_{111} has returned to a large negative value. This establishes one more point important for development of an understanding of the elastic behavior of a material undergoing an intermediate-valence transition. As the transition is approached from the high-volume side, the interatomic repulsive forces decrease but once the transition has been completed the large repulsive force between nearest neighbors comes back into play and determines the higher-order elasticity in the metallic state.

ACKNOWLEDGMENTS

We are most grateful to J. Penfold and G. D. Pitt for allowing us to use the United Kingdom Science and Engineering Research Council (SERC) high-pressure facilities at Standard Telecommunications Laboratories Limited, Harlow, and to Professor S. Methfessel for encouragement of the work.

---

[1] A. Jayaraman, V. Narayamanurti, E. Bucher, and R. G. Maines, Phys. Rev. Lett. 25, 1430 (1970).

[2] R. I. Melcher, G. Güntherodt, T. Penney, and F. Holtzberg, IEEE Trans. Sonics Ultrason. 11, 616 (1975).

[3] T. Penney, R. L. Melcher, F. Holtzberg, and G. Güntherodt, in *Magnetism and Magnetic Materials—1975 (Philadelphia),* Proceedings of the 21st Annual Conference on Magnetism and Magnetic Materials, edited by J. J. Becker, G. H. Lander, and J. J. Rhyne (AIP, New York, 1976), p. 392.

[4] G. A. Saunders, W. A. Lambson, Tu. Hailing, D. W. Bullet, H. Bach, and S. Methfessel, J. Phys. C 15, L551 (1982).

[5] S. Methfessel and D. C. Mattis, *Encyclopedia of Physics,* edited by S. Fluge (Springer, Berlin, 1968), p. 389.

[6] S. I. Xhao, Phys. Rev. B 1, 4589 (1970).

[7] G. Güntherodt, P. Wachter, and D. M. Imboden, Phys. Kondens. Mater. 12, 292 (1971).

[8] B. Batlogg, E. Kaldis, A. Schlegel, and P. Wachter, Phys. Rev. B 14, 5503 (1976).

[9] P. Wachter, Solid State Commun. 7, 693 (1969).

[10] E. Kaldis and P. Wachter, Solid State Commun. 11, 907 (1972).

[11] V. Narayanamurti, A. Jayaraman, and E. Bucher, Phys. Rev. 9, 2521 (1974).

[12] J. L. Kirk, K. Vedam, V. Narayanamurti, A. Jayaraman, and E. Bucher, Phys. Rev. B 6, 3023 (1972).

[13] A. Chatterjee, A. K. Singh, and A. Jayaraman, Phys. Rev. B 6, 2285 (1972).

[14] L. L. Hirst, Phys. Kondens. Mater. 11, 255 (1970).

[15] M. B. Maple and D. Wohlleben, Phys. Rev. Lett. 27, 511 (1971).

[16] F. Mehren, J. B. Torrance, and F. Holtzberg, Phys. Rev. B 8, 1268 (1973).

[17] F. Holtzberg, in *Magnetism and Magnetic Materials—1973 (Boston),* Proceedings of the 19th Annual Conference on Magnetism and Magnetic Materials, edited by C. D. Graham and J. J. Rhyne (AIP, New York, 1974), p. 478.

[18] A. Jayaraman, E. Bucher, P. Dernier, and L. D. Longinotti, Phys. Rev. Lett. 31, 700 (1973).

[19] A. Jayaraman, P. Dernier, and L. D. Longinotti, Phys. Rev. B 11, 2783 (1975).

[20] R. A. Pollak, F. Holtzberg, J. L. Frecouf, and D. E. Eastman, Phys. Rev. Lett. 33, 820 (1974).

[21] R. A. Cowley, Phys. Rev. B 13, 4877 (1976).

[22] H. Boppart, A. Treindl, and P. Wachter, *Valence Fluctuations in Solids,* edited by L. M. Falicov, W. Hanke, and M. B. Maple (North-Holland, Amsterdam, 1981), p. 103.

[23] H. Boppart, W. Rehwald, E. Kaldis, and P. Wachter, International Conference on Valence Instabilities, Zürich, 1982 (unpublished).

[24] W. Kress, H. Bilz, G. Güntherodt, and A. Jayaraman, J. Phys. (Paris) Colloq. 42, C6-3 (1981).

[25] F. Levy and P. Wachter, Solid State Commun. 8, 183 (1970).

[26] H. Bilz, G. Güntherodt, W. Kleppman, and W. Kress, Phys. Rev. Lett. 43, 1998 (1979).

[27] A. Jayaraman, B. Batlogg, R. G. Maines, and H. Bach, Phys. Rev. B 26, 3347 (1982).

[28] Y. K. Yoğurtçu, E. F. Lambson, A. J. Miller, and G. A. Saunders, Ultrasonics 18, 155 (1980).

[29] R. N. Thurston and K. Brugger, Phys. Rev. 133, A1604 (1964).

[30] A. J. Miller, G. A. Saunders, and Y. K. Yoğurtçu, J. Phys. C 14, 1569 (1981).

[31] C. M. Varma, Rev. Mod. Phys. 48, 219 (1976).

[32] O. L. Anderson and R. C. Liebermann, Phys. Earth Planet Inter. 3, 61 (1970).

[33] R. Keller, G. Güntherodt, W. B. Holzapfel, M. Dietrich, and F. Holtzberg, Solid State Commun. 29, 753 (1979).

[34] J. K. Liakos and G. A. Saunders, Philos. Mag. A 46, 217 (1982).

[35] M. P. Brassington and G. A. Saunders, Phys. Rev. Lett. 48, 159 (1982).

[36] O. L. Anderson and J. E. Nafe, J. Geophys. Res. 70, 3951 (1965).

[37] K. S. Krishnan and S. K. Roy, Proc. R. Soc. London, 210, 481 (1952).

[38] P. B. Ghate, Phys. Rev. 139, A1666 (1965).

[39] K. Brugger and T. C. Fritz, Phys. Rev. 157, 524 (1967).

[40] A. Jayaraman, A. K. Singh, A. Chaterjee, and U. Devi, Phys. Rev. B 9, 2513 (1974).